

Design of High Precision CNC Vertical Lathe Turning Tool Holder

Wenwu ZHANG, Guangchen XU, Lin QIAN, Mantong WANG*

Yingkou Institute of Technology, Yingkou, Liaoning, 115000, China

*Corresponding Author: Jiayu LI, E-mail: 13509779@qq.com

Abstract:

A large aspect ratio vibration reducing tool holder based on passive damping vibration reduction technology is designed to solve the vibration problem that occurs in deep hole machining of vertical lathes. A dynamic model of passive damping vibration reduction tool holder was established, and the optimal damping ratio, optimal frequency ratio, and maximum relative amplitude were derived. Modal analysis of the passive damping vibration reduction tool holder was conducted using software. The results showed that the maximum response amplitude of the passive damping vibration reduction tool holder decreased significantly compared to the original one.

Keywords: CNC vertical lathe; Cutting chatter; Cutting tool holder

1 Introduction

Mechanical manufacturing is an important industry in today's society and a pillar industry for China's economic development, social progress, and national defense industry. The accuracy, efficiency, quality, and economy of mechanical processing are intuitive manifestations of the level of national manufacturing industry.

Since the 20th century, China has gradually become a major manufacturing country and a world OEM factory. However, there is still a significant gap in the overall level of high-end manufacturing between China and countries such as Europe and America. The gap between manufacturing powers and manufacturing powers is a challenge that we need to overcome. The reason for this dilemma is the gap in mechanical manufacturing equipment in China. With the continuous development of mechanical manufacturing equipment, the requirements for high-precision machining level and precision machining technology in mechanical processing are constantly increasing.

Among the overall stiffness of CNC vertical lathes, the vertical tool holder has the lowest stiffness, with large cutting volume or vertical ram extension length, which can cause vibration during machining, leading to a decrease in workpiece machining accuracy, reduced surface smoothness, and even tool breakage. This project is based on the design of the VCT16-NC CNC vertical lathe turning tool holder. On this basis, a dynamic model of the damping dynamic damping slider is established, and the damping dynamic damping technology is used to

analyze the damping dynamic damping of the VCT16-NC CNC vertical lathe turning tool holder. Using anti vibration theory, improve the cutting stiffness of the vertical tool holder, and achieve a length to diameter ratio (the ratio of the extended length of the slider to the interface edge length of the slider) greater than "5" or greater under the maximum cutting force state of the slider without generating cutting chatter. To achieve many advantages such as improving machining accuracy, surface smoothness, seismic resistance, and machining efficiency, if the research results of this project are promoted and used in the machine tool industry, economic and social benefits will be obtained.

In recent years, domestic and foreign scholars have conducted extensive research on machining chatter, and have recognized that taking certain measures to reduce or eliminate tool vibration is an important method to ensure machining quality. At present, the main directions for applying damping and vibration reduction include the damping system of Taipei 101 Building, the damping and vibration reduction boring bar of Swedish Sandvik Company, and the damping system applied in the high-speed rail field. We take the damping and vibration reduction boring bar of Swedish Sandvik Company as the research object to complete the vibration reduction design of the turning tool holder.

Cutting chatter is a mechanical vibration generated during the machining process, which can affect the accuracy and surface roughness of the workpiece, accelerate the wear of machine tools, and reduce production efficiency. During the machining process, cutting chatter is inevitable, and the tool rest ram is the

weakest part of the lathe tool rest in terms of stiffness. During the production process, the larger the aspect ratio of the tool rest ram, the lower its stiffness, and the easier it is to generate cutting chatter. To reduce the impact of cutting chatter on machining, a damping damper is placed in the inner cavity of the tool rest ram, By damping the relative vibration between the shock absorber and the knife rest ram, the kinetic energy of the knife rest ram vibration is consumed, thereby achieving the effect of vibration reduction.

2 Theoretical Model Establishment of Vibration Damping Ram

2.1 Structural design of damping dynamic damping ram

The damping dynamic damping ram consists of two parts: a knife rest ram and a damping system, where the damping system consists of damping fluid, damping blocks, and circular rubber rings. The damping fluid surrounds between the damping block and the annular rubber ring, providing resistance to the movement of the damping block. The damping block in the damping system is used as a "vibration core" throughout the entire ram. According to the theory of vibration absorbers, the heavier the mass block, the more obvious the damping effect. Therefore, the vibration core material is high-density hard alloy. The annular rubber ring is installed at both ends of the damping block as a support component to provide support for the damping block, ensuring that there is no contact or elastic collision between the damping block and the ram. The annular rubber ring has a high elastic modulus, and within its elastic range, the radial deformation of the annular rubber ring can provide a certain spring stiffness for the damping block, and has a certain linear relationship with the load it is subjected to. During the machining process, the ram is subjected to impact loads, resulting in cutting chatter. The internal vibration core generates forced vibration, and the damping system begins to work, absorbing the kinetic energy of the ram vibration, thereby playing a role in vibration reduction.

2.2 Simplified model of damping ram

The force analysis of the original model of the ram can be divided into two types: radial force and torque. The position of the ram near the tool holder is analyzed, and the influence of torque on the model is relatively small. It is ignored here. In the process of studying the damping ram, an equivalent substitution method is used to select the center position of the damping block as the research object, and the mass of the damping block is equivalent in this regard, Equivalent the mass of the ram to a mass block acting on the point we are studying, and equivalent the spring stiffness provided by the annular rubber ring to the equivalent elastic coefficient at the

research point. Establish a dynamic model of the damping ram:

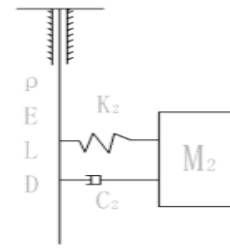


Figure 1 Original model of the ram

ρ —Material density of the ram; E —Elastic modulus of ram material; L —The elongation length of the ram during operation; K —Equivalent spring stiffness at the research point; K_1 —Equivalent stiffness coefficient of annular rubber ring; D —Dimensions of the ram interface; C_2 —Damping coefficient of ram damping fluid; M_2 —Mass of damping block

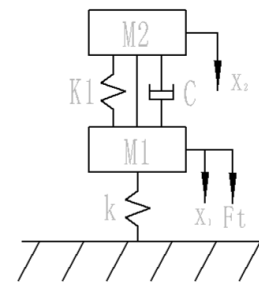


Figure 2 Dynamic model of damping ram

For the convenience of our research, we found that the motion mode of the damping ram is the same as that of the damping boring bar. Therefore, we equivalent the damping ram to an enlarged damping boring bar. Due to the complexity of the dynamic calculation of the damping ram, we use the formula in [1] to calculate it. We assume that only one impact load $F_{(t)} = Fe^{i\omega t}$ acts on M_1 and establish the following equation based on Newton's second law:

$$\begin{cases} M_1 \ddot{X}_1 + c(\dot{X}_1 - \dot{X}_2) + K_1(X_1 - X_2) + KX_2 = F_{(t)} \\ M_2 \ddot{X}_2 - c(\dot{X}_1 - \dot{X}_2) - K_1(X_1 - X_2) = 0 \end{cases} \quad (1)$$

Solved:

$$\begin{cases} x_1 = B_1 \exp[i(\omega t - \varphi_1)] \\ x_1 = B_2 \exp[i(\omega t - \varphi_2)] \end{cases} \quad (2)$$

The first and second derivatives are:

$$\begin{cases} \dot{x}_1 = iB_1\omega \exp[i(\omega t - \varphi_1)] \\ \ddot{x}_1 = -B_1\omega^2 \exp[i(\omega t - \varphi_1)] \end{cases} \quad (3)$$

$$\begin{cases} \dot{x}_2 = iB_2\omega \exp[i(\omega t - \varphi_2)] \\ \ddot{x}_2 = -B_2\omega^2 \exp[i(\omega t - \varphi_2)] \end{cases} \quad (4)$$

Substitute its first and second derivatives into equation system:

$$\begin{cases} [k + k_1 - M_1\omega^2 + i\omega c]B_1 \exp[i(\omega t - \varphi_1)] - (k_1 + i\omega c)B_2 \exp[i(\omega t - \varphi_2)] = F \exp(i\omega t) \\ [k_1 - M_2\omega^2 + i\omega c]B_2 \exp[i(\omega t - \varphi_2)] - (k_1 + i\omega c)B_1 \exp[i(\omega t - \varphi_1)] = 0 \end{cases} \quad (5)$$

Expressed in matrix form as:

$$\begin{pmatrix} k + k_1 - m_1\omega^2 + i\omega c & -(k_1 + i\omega c) \\ -(k_1 + i\omega c) & k_1 - m_1\omega^2 + i\omega c \end{pmatrix} \begin{Bmatrix} B_1 \exp(-i\varphi_1) \\ B_2 \exp(-i\varphi_2) \end{Bmatrix} = \begin{Bmatrix} F \\ 0 \end{Bmatrix} \quad (6)$$

The amplitude expression is: $k = m\omega_n^2 = 238868 \text{ N/mm}$
Obtain:

$$\begin{cases} B_1 \exp(-i\varphi_1) = \frac{(k_1 - m_1\omega^2 + i\omega c)F}{(k + k_1 - m_1\omega^2 + i\omega c)(k_1 - m_2\omega^2 + i\omega c) - (k_1 + i\omega c)^2} \\ B_2 \exp(-i\varphi_2) = \frac{(k_1 + i\omega c)F}{(k + k_1 - m_1\omega^2 + i\omega c)(k_1 - m_2\omega^2 + i\omega c) - (k_1 + i\omega c)^2} \end{cases} \quad (7)$$

Solve out B_1, B_2 , expression:

$$\begin{cases} B_1 = \frac{F\sqrt{(k_1 - \omega^2 m_2)^2 + (\omega c)^2}}{\sqrt{[(k - \omega^2 m_1)(k_1 - \omega^2 m_2) - \omega^2 m_2 k_1]^2 + [(\omega c)(k - \omega^2 m_1 - \omega^2 m_2)]^2}} \\ B_2 = \frac{F\sqrt{(k_1)^2 + (\omega c)^2}}{\sqrt{[(k - \omega^2 m_1)(k_2 - \omega^2 m_2) - \omega^2 m_2 k_1]^2 + [(\omega c)(k - \omega^2 m_1 - \omega^2 m_2)]^2}} \end{cases} \quad (8)$$

$$\left(\frac{B_1}{\delta_{st}}\right)^2 = \frac{(a^2 - \lambda^2)^2 + (2\xi\alpha\lambda)^2}{[(1 - \lambda^2)(a^2 - \lambda^2) - \mu\lambda^2 a^2]^2 - (2\xi\alpha\lambda)^2(1 - \lambda^2 - \mu\lambda^2)^2} \quad (9)$$

$$\left(\frac{B_2}{\delta_{st}}\right)^2 = \frac{\alpha^4 + (2\xi\alpha\lambda)^2}{[(1 - \lambda^2)(a^2 - \lambda^2) - \mu\lambda^2 a^2]^2 + (2\xi\alpha\lambda)^2(1 - \lambda^2 - \mu\lambda^2)^2} \quad (10)$$

Do variable substitution:

$$\omega_{n1} = \sqrt{\frac{K}{M_1}}, \quad \omega_{n2} = \sqrt{\frac{K_1}{M_2}}, \quad \mu = \frac{M_2}{M_1}, \quad \alpha = \frac{\omega_{n2}}{\omega_{n1}}, \quad \xi = \frac{c}{2\sqrt{m_2 K_1}}$$

$$\lambda = \frac{\omega}{\omega_{n1}}, \quad x_{st} = \frac{F e^{i\omega t}}{K} \quad (11)$$

The relative displacement expression of the replaced damping ram:

$$S = \sqrt{\frac{(\alpha^2 - \lambda^2)^2 + 4\alpha^2 \xi^2 \lambda^2}{[(1 - \lambda^2)(\alpha^2 - \lambda^2) - \mu\alpha^2 \lambda^2]^2 + 4\alpha^2 \xi^2 \lambda^2 (1 - \lambda^2 - \mu\lambda^2)^2}} \quad (12)$$

2.3 Relative displacement and frequency curve of damping ram

In the function of S about α, μ, λ and ξ , using ξ as a variable, order $\alpha=0.916$, order $\mu=0.0915$. Draw the relative amplitude to frequency ratio curve of the damping ram in MATLAB software:

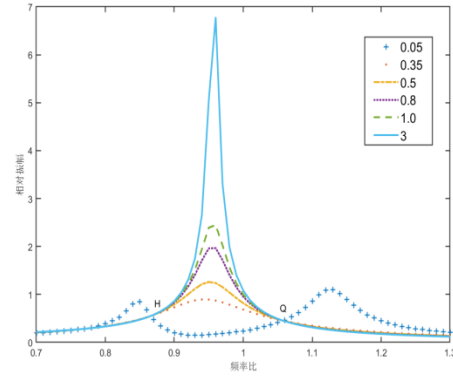


Figure 3 Curve of relative displacement to frequency ratio

In the figure, we can see that the curves of curve a under different damping conditions intersect at two points b and c. Regardless of the damping value, the relative displacement to frequency ratio curve passes through H and K. Therefore, the properties of these two points are independent of the magnitude of the damping ratio. Substituting $a=0$ and $b=\infty$ into function S respectively yields:

$$\begin{cases} S_0 = \frac{(\alpha^2 - \lambda^2)}{(1 - \lambda^2)(\alpha^2 - \lambda^2) - \mu\alpha^2 \lambda^2} \\ S_\infty = \frac{1}{(1 - \lambda^2 - \mu\lambda^2)} \end{cases} \quad (13)$$

The intersection point of the S_0 and S_∞ amplitude curves, namely the H and K points. Due to the opposite response of and, there are:

$$\frac{\alpha^2 - \lambda^2}{(1 - \lambda^2)(\alpha^2 - \lambda^2) - \mu\alpha^2 \lambda^2} = \frac{-1}{(1 - \lambda^2 - \mu\lambda^2)} \quad (14)$$

$$\text{Obtain: } \alpha = \frac{1}{1 + \mu}$$

2.4 Solution to the optimal damping ratio

At the highest point of the H and K curves, make

$$\frac{\partial S^2}{\partial \lambda^2} = 0, \quad \frac{h}{k} = \frac{1}{[1 - \lambda^2 - \mu\lambda^2]^2}$$

Find the optimal damping ratio of the damping ram

$$\text{as: } \xi = \sqrt{\frac{3\mu}{8(1 + \mu)}}$$

3 Parameter Calculation of Damping Ram

Add local contact without penetration to the eight diagonal iron and the contact surface between the iron and the sliding pillow at the upper and lower ends of the tool holder, and add fixed constraints on the back. Apply tangential cutting force at the top of the sliding pillow, and conduct finite element analysis on the maximum elongation of the hollow vibration damping sliding pillow vertically, as shown in Figure 4:

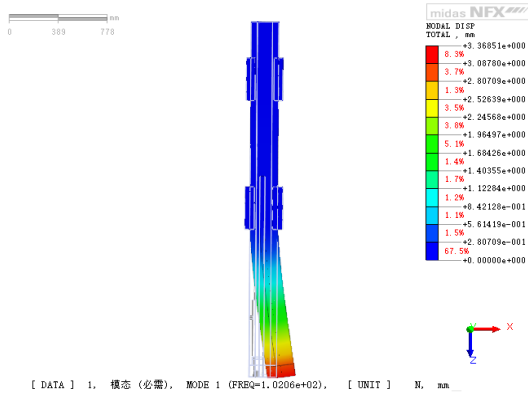


Figure 4 Modal Frequency Response Diagram

In the figure, we can see that the first-order modal resonance frequency of the damping ram is $f = 102.06 \text{ Hz}$.

3.1 Main parameter calculation

We can calculate the natural vibration angular frequency of the damping ram through first-order modal analysis as follows:

$$\omega_N = 2\pi f = 640.88 \text{ rad/s} \quad (15)$$

Here we use software to calculate the masses M_1 and M_2 of the ram and damping block: $M_1 = 757.46 \text{ Kg}$, $M_2 = 69.31 \text{ Kg}$

The mass ratio of the damping ram is:

$$\mu = \frac{M_2}{M_1} = \frac{69.31}{757.46} = 0.0915 \quad (16)$$

Natural frequency ratio: $\alpha = \frac{1}{1 + \mu} = 0.916$

The homology frequency ω_n is:

$$\omega_n = \alpha \cdot \omega_N = 587.05 \text{ rad/s} \quad (17)$$

The equivalent stiffness K of the shock absorber mirror rod is:

$$K = M\omega_n^2 = 311109405 \text{ N/mm} \quad (18)$$

The stiffness K of the power absorber is:

$$K = M\omega_n^2 = 23886.8 \text{ N/mm} \quad (19)$$

optimal damping ratio: $\xi = \sqrt{\frac{3\mu}{8(1+\mu)}} = \sqrt{\frac{3 \times 0.0915}{8 \times 1.0916}} = 0.177$

The damping of the power absorber can be obtained as:

$$c = 2\xi m\omega_n = 14403.95 \text{ N} \cdot \text{s/m} \quad (19)$$

3.2 Selection of damping fluid

The magnitude of the damping coefficient of the damping fluid depends on the viscosity of the damping fluid, which is calculated using the kinematic viscosity in

$$\text{reference}^{[1]} \nu = \frac{\mu}{\rho} = \frac{c}{128lp}$$

By searching for literature, it has been found that methyl silicone oil has good damping properties and various physical and chemical properties, which can provide a large damping coefficient. Therefore, methyl silicone oil is used

as the damping fluid for the damping ram.

4 Simulation of Vibration Damping Ram

4.1 Establishing a simulation analysis model for damping dynamic vibration damping sleepers

We have chosen the Midas NFX finite element analysis software to analyze the vibration damping ram. In the process of establishing a simulation model of the damping dynamic vibration damping ram, we should try to restore the movement of the ram under real conditions as much as possible. The work of the ram cannot be separated from the precise fit of components such as the slide seat, balance cylinder, and rolling screw. If we model and analyze all components such as the slide seat, balance oil cylinder, and rolling screw when establishing a simulation analysis model for damping dynamic vibration reduction sleepers, it will greatly increase our workload and work difficulty. Therefore, we need to simplify the simulation analysis model of the damping ram while meeting the actual working conditions of the ram. (The slide seat is a fixed inclined iron and a support iron that wrap around the sliding pillow. The use of a balance oil cylinder is to reduce the driving force of the motor, and the ball screw is the driving element, which has a relatively small impact on the sliding pillow when it is at its maximum extended stroke.) The following principles should be followed: ① The stiffness of the damping ram should not be lower than the maximum stiffness required for actual operation; ② The damping fluid between the damping ram and the internal damping system is replaced by linear damping; ③ Except for the damping ram and its built-in damping system, all other parts are considered rigid bodies; The overall analysis model of the damping ram is shown in the figure 5:



Figure 5 Finite element root system model diagram

4.2 Finite element analysis process of vibration damping ram

4.2.1 Material of damping ram

According to the original VCT16-NC CNC vertical lathe, the material used for turning the tool holder slider is 45 steel. The damping block in the built-in damping system of the slider should be made of materials with higher mass density. Among the metal materials, tungsten has a higher mass density, and the mass density of tungsten alloy can reach 19.3 g/cm^3 . All its properties

meet the working conditions of the damping block. Therefore, tungsten based heavy alloy is chosen as the material with fast damping.

4.2.2 Add constraint

In the simplified model of the tool holder, due to the mutual contact between the damping ram and the slide seat, which is not completely in contact, 16 columns are used as the simplified model of the slide seat. In order to better analyze the damping effect of the slide seat, the simplified model of the slide seat is a rigid body and fixed, and bidirectional sliding is added between the damping ram and the slide seat. As shown in the figure 6:

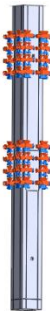


Figure 6 Analysis Model Constraint Diagram

4.3 Finite element analysis of damping dynamic damping sleeper

In order to visually demonstrate the vibration reduction effect of the damping ram, we used modal analysis method for transient response analysis and conducted comparative experiments between the original tool holder ram and the damping ram. An impact load was applied at the connection of the tool fixture between the original tool holder ram and the damping ram, and the damping ram vibrated after being subjected to the impact load. The vibration amplitude of the two types of rams was observed. In Figure 7, we can visually see the vibration reduction effect of the damping damping ram.



Figure 7 Comparative Test

5 Conclusion

The improvement design of the vertical lathe turning tool holder components analyzed and summarized the problems of machining accuracy and surface smoothness caused by cutting chatter in the processing equipment. A damping dynamic damping ram was designed, and the optimization design and finite element analysis of the damping dynamic damping ram were carried out to minimize the amplitude and frequency of cutting chatter generated during the machining process of the vertical lathe tool holder components.

Fund Projects: ① Science and Technology Research Project of Liaoning Provincial Department of Education: Research on the Application of Damping and Vibration Reduction Technology in Key Components of Machine Tools; (JYTMS20230066) ② The Fund of Liaoning Provincial Natural Science and Technology Foundation Regional Joint (No.2021-YKLH-08).

References

- [1] Qin Bai. Study on Dynamic Characteristics Simulation and Optimization Design of Dynamical Vibration Absorption Boring Bar with Damping [J]. Harbin University of Science and Technology, 2009(24):11-19.
- [2] Hou Xueyuan, Ren Xueoing, Ren Chong. Structure Design and Dynamic Characteristic Simulation Study of a Vibration Damping Boring Cutter [J]. MACHINE TOOL&HYDRAULICS, 2010(47):21-25.
- [3] Yang Liyu. Optimization Design and Simulation Study of Particle Damping and Magnetorheological Composite Damping Boring Cutter [D]. North University, 2018.
- [4] He Miao. Dynamic Characteristics Analysis and Optimization Design of Dynamic Damping Boring Bar [D]. Southeast University For the Academic Degree of Master of Engineering, 2018.
- [5] Du Jingxuan. Study on Theory and Experiments for Damping Tools with High Slenderness Ratio [D]. North University, 2013, 4(12):25-29.
- [6] Shen Xingquan, Ma teng, Gao Weijia. Research on Flutter Suppressing Device of Deep Hole Machining Based on Magnetorheological Effects [J]. 2017(12):45-19.
- [7] Liu Lijia, Liu Xianl. Comprehensive survey of vibration control technology in machining [J]. International Journal of Hybrid Information Technology, 2015, 8(4):307-316.